
Article:
Lad, U, Kale, GM and Bryaskova, R (2014) Sarcosine Oxidase Encapsulated Polyvinyl Alcohol-Silica-AuNP Hybrid Films for Sarcosine Sensing Electrochemical Bioelectrode. Journal of The Electrochemical Society, 161 (5). B98-B101. ISSN 0013-4651

https://doi.org/10.1149/2.018405jes

Sarcosine Oxidase Encapsulated Polyvinyl alcohol-Silica-AuNP Hybrid Films for Sarcosine Sensing Electrochemical Bioelectrode

Umesh Lad[a], Girish M. Kale[a,*], and Rayna Bryaskova[b].

[a] *Institute for Materials Research, SPEME, University of Leeds, Leeds LS2 9JT, UK*
[b] *University of Chemical Technology and Metallurgy, Department of Polymer Engineering, 8 Kl. Ohridski, 1756 Sofia, Bulgaria*
Author for all correspondences. Email: g.m.kale@leeds.ac.uk; Tel: 0044-113-3432805

The amperometric response of sarcosine was measured in aqueous media containing ferrocene monocarboxylic acid using the redox enzyme sarcosine oxidase (SOD) immobilized in a composite material based on polyvinyl alcohol (PVA) and partially prehydrolyzed tetraethyl orthosilicate (pphTEOS) at the surface of "in-house" fabricated graphite electrodes. For comparison, separate electrodes consisting of silver and gold nanoparticles (Ag/AuNPs) embedded in the PVA-pphTEOS matrix was prepared employing a novel sol-gel process based on the in situ chemical reduction of Ag or Au ions using PVA both, as a reducing agent and stabilizer. The analytical performance of the enzyme electrodes was studied in terms of linear ranges, sensitivities, response times, limits of detection, reproducibility and stability.

Untreated or uncontrolled type II diabetes can lead to serious health complications such as diabetic nephropathy, cardiovascular disease, stroke and blindness. According to the National Health Service (U.K.), diabetic nephropathy is the most common cause of chronic kidney disease with half of all cases caused by diabetes and just over a quarter of cases due to high blood pressure. When kidney disease is caused by diabetes the problems advance more quickly and progress more rapidly than other causes such as high blood pressure or ageing of the kidneys. Diabetic nephropathy occurs from the damage of the nephrons in the kidneys from the build up of blood glucose, which in turn, affects the kidneys to filter out waste products and fluids. Creatinine is naturally produced by the body through the metabolism of creatine phosphate in muscle and is filtered from the bloodstream by the kidneys in relatively constant amounts every day. Plasma concentration of the waste substance creatinine is a reasonable indicator of renal function.

A review by Lad et al[1] shows that electrochemical biosensors for determining creatinine in blood serum is essential for the point of care treatment and management of the kidney malfunction condition. Most potentiometric sensors use gas-selective or pH-sensitive electrodes covered with an immobilized creatininie iminohydrolase or creatinine deiminase membrane that catalyses the biochemical reaction. The majority of amperometric biosensors rely on the three-enzyme method first described by Tsuchida and Yoda.[2] This involves the hydrolysis of creatinine using creatininase (CA), creatinase (CI) and sarcosine oxidase (SOD) in a three-stage enzyme-catalyzed reaction sequence. The last step of the sequence involves the flavin-containing enzyme SOD, which reacts as follows:

$$\text{Sarcosine} + \text{SOD}(FAD^+) \longrightarrow \text{Glycine} + \text{Formaldehyde} + \text{SOD}(FADH_2) \quad (1)$$

$$\text{SOD}(FADH_2) + O_2 \longrightarrow \text{SOD}(FAD^+) + H_2O_2 \quad (2)$$

$$H_2O_2 \longrightarrow 2H^+ + O_2 + 2e^- \quad (3)$$

In the above reactions, FAD^+ and $FADH_2$ are the oxidized and reduced forms of flavin adenine dinucleotide respectively. Oxidation and reduction of the FAD moiety can be achieved using O_2 as in the first-generation biosensor; an artificial redox mediator molecule as in the second-generation biosensor; or meadiatorless approach as in the third-generation biosensor. The most popular approach based on the above scheme is to monitor the generation of H_2O_2. This mode of operation involves regeneration of O_2 from the electrochemical oxidation of H_2O_2, which then completes with the enzyme cycle (reaction 3). The major problem with these biosensors is their dependency on the concentration of dissolved oxygen. Alternatively, an electron mediator (Med) could be used in place of O_2 to regenerate the enzyme $SOD(FAD^+)$.[3,4] Third-generation biosensors have

the enzymes' active site in direct contact with the electrode to ensure direct electron transfer and commonly achieved with the use of nanoparticles. To date, many efforts have been made to investigate the direct electrochemistry of other redox enzymes however; to the best of our knowledge the direct electrochemistry of SOD has only recently been reported.[5] Zhou et al immobilized SOD on graphene, chitosan and silver nanoparticles modified glassy carbon to study the direct electrochemistry of the enzyme.

Recently our group presented the detailed characterization for the immobilization of glucose oxidase (GOD) within PVA-TEOS matrix at an "in-house" fabricated graphite electrode for the determination of glucose.[6] Enzyme electrodes were also prepared using NPs embedded in the PVA-TEOS matrix prepared. From our preliminary work we found that akin to GOD, SOD was chemically stable and was not susceptible to hydrolysis reaction upon addition to the PVA-TEOS mixture prior to immobilization. Therefore, in this communication we present a logical extension to the previously conducted research work[6] that involves the immobilization of SOD within PVA-TEOS matrix at the surface of an "in-house" fabricated graphite electrode for the determination of sarcosine. We also prepared Ag and AuNPs embedded in the PVA-TEOS matrix employing a sol-gel process based on the in situ reduction of Ag or Au ions using PVA as a reducing agent as well as a nanoparticle suspension stabilizer.

Experimental

Reagents and materials. – Polyvinyl alcohol (PVA, 87-89% hydrolyzed, average MW = 13000-23000, Sigma-Aldrich), tetraethyl orthosilicate (TEOS, ≥99.0%, Aldrich), nitric acid (HNO_3, 2.0 M, Riedel-de Haën), silver nitrate ($AgNO_3$, AcrosOrganics), auric chloride ($HAuCl_4$, 99.99%, Aldrich), graphite rod (99.99%, Goodfellows), sarcosine oxidase (SOD, from *Bacillus sp.*, 49 U mg^{-1}, Sigma-Aldrich), sarcosine (Sigma-Aldrich), ferrocene monocarboxylic acid (FMCA, ≥97.0%, Fluka) and phosphate buffer solution (PBS, 1.0 M, pH 7.0, Sigma-Aldrich) were used in respective experiments as supplied by the supplier without any further purification. Deionized water (Milli-Q) was used in all experiments.

All glassware was cleaned in freshly prepared HNO_3/HCl (1:3) solution, thoroughly rinsed with deionized water and dried before use.

Preparation of PVA-Ag/AuNPs and pphTEOS. – In a typical synthesis, PVA solution (5%) was prepared by dissolving 5.0 g of PVA in 95 mL of water under magnetic stirring and heating to 80 ^oC for 30 min in order to obtain a colourless PVA solution.

To obtain AgNPs, $AgNO_3$ (500 mg dissolved in 0.5 mL water) was added to 25 mL PVA (5%), stirred and heated for 1 hr at 100 ^oC under reflux. The colour of the solution in the resulting sample deepens gradually from an achromatic colour in the beginning to a deep yellow-brownish equilibrium colour. To retain a stable Ag colloid structure consisting of AgNPs capped in PVA molecules, the samples were cooled to 20-25 ^oC temperature just after the reaction and before employing for further experimentation. For PVA-AuNPs composites, $HAuCl_4$ (10 mg dissolved in 0.5 mL water) was added to 25 mL PVA (5%), stirred and heated for 1 hr at 100 ^oC under reflux. The pale yellow colour in the beginning slowly changes to purple before settling at a deep red colour. All composite solutions were stored in dark bottles at 4 ^oC.

A homogenous standard of pphTEOS was prepared under magnetic stirring of 1 mL TEOS, 1mL water and 0.1 mL of HNO_3 in a small vial at room temperature for 60 min. Next, an aliquot of pphTEOS (0.3 mL) and 5% PVA (1 mL) solutions were mixed thoroughly under magnetic stirring. The solution mixture was freshly prepared prior to the fabrication of every enzyme electrode. Precalibrated micropipettes were used for accurately measuring the reagent solutions during the synthesis process.

Preparation of the graphite electrode and immobilization of sarcosine oxidase. – The "in-house" fabricated graphite rod electrode surfaces (area = 0.196 cm^2) were treated on (1) p660 then (2) p1200 grade of emery paper, and brought to an almost mirror like finish by polishing on (3) 80 g m^{-2} paper. The graphite electrodes were reused after polishing through steps (1)–(3) as described. Prior to any modifications, the electrodes were cycled between -0.5 and +1.2 V (*vs.* Ag/AgCl) at 50 mV s^{-1} in 0.1 M PBS (pH 7.0) until a stable profile was obtained.

A 20 μL aliquot solution of PVA-pphTEOS (volume ratio 1:0.3 respectively) and a 5 μL aliquot of SOD (10 U μL^{-1}) was mixed in an ultrasonic bath for 1 min to accelerate the dispersion of the enzyme in the pphTEOS and PVA mixture. Subsequently, a 5 μL sample of this mixture was spread over the surface of the graphite electrode followed by drying in air for 24 hr. The resulting electrodes were denoted as PVA-pphTEOS-SOD. Alternatively, Ag or AuNPs electrodes (denoted as PVA-Ag/AuNPs-pphTEOS-SOD) were fabricated using a similar method except that it included PVA containing Ag or AuNPs respectively. TEM images of the NPs are shown in Figure 1. All the enzyme electrodes were stored at 4 ^{o}C when not in use.

112

(A)

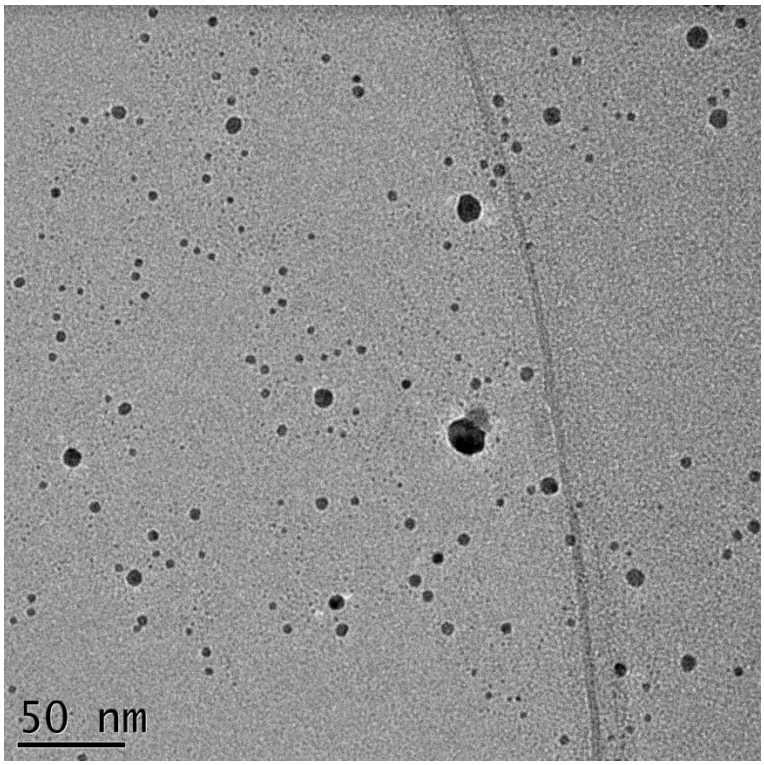

(B)

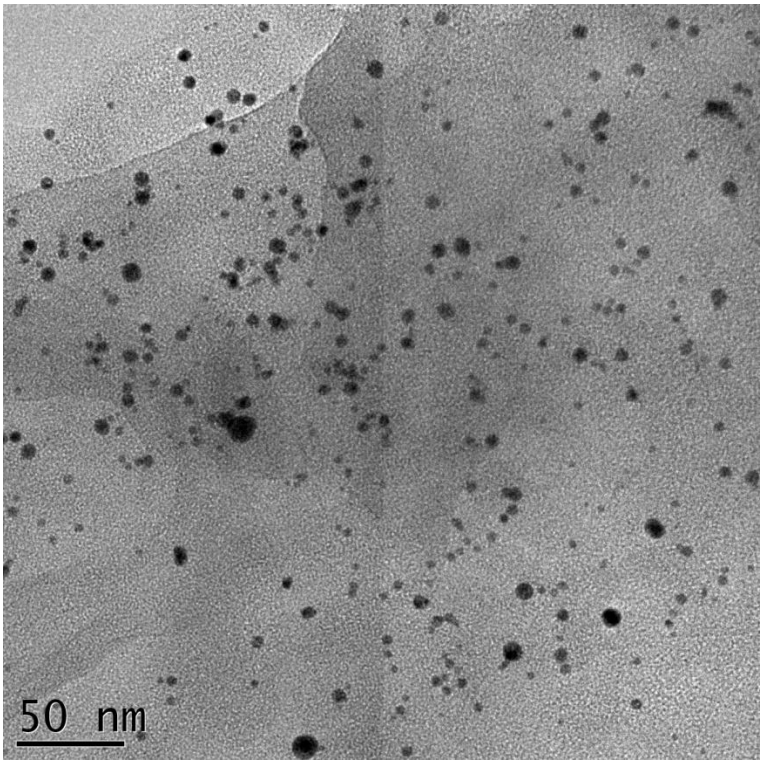

Figure 1A and Figure 1B

113

114 Figure 1. TEM images of (A) PVA-Ag-pphTEOS and (B) PVA-Au-pphTEOS films.

115

116 *Apparatus and electrochemical measurements.* – All electrochemical experiments were performed
117 with the computer controlled SI1287 Electrochemical Interface (Solartron, U.K.) at 25 ^{o}C with a conventional
118 50 mL three-electrode system compromising of a platinum wire auxiliary (Model XM110, Radiometer
119 Analytical), Ag/AgCl (3.0 M KCl) reference (Model REF321, Radiometer Analytical) and "in-house" fabricated

graphite rod as the working or sensing electrodes. The amperometric and cyclic voltammetric detection of sarcosine were performed in nitrogen purged solutions of PBS (0.2 M) in the presence or absence of FMCA (0.8 mM). A magnetic stirrer and stirrer bar provided the convective transport during the *current-time* (*I-t*) amperometric studies.

Results and Discussion

Electrochemical characterization of the PVA-pphTEOS-SOD composite films: mechanism of sarcosine determination and influence of buffer pH. – Figure 2 (curve *a*) shows the cyclic voltammogram of the PVA-pphTEOS-SOD graphite electrode in 0.2 M PBS (pH 7.0) where no visible reaction is taking place. However, in the presence of 0.8 mM FMCA, a pair of reversible cyclic voltammetric peaks appeared (curve *b*). These peaks are assigned to one electron redox reaction of $FMCA^{+}$/FMCA couple. Upon introducing sarcosine to the buffer solution containing FMCA, well-defined catalytic reaction waves are observed (curves *c-e*).

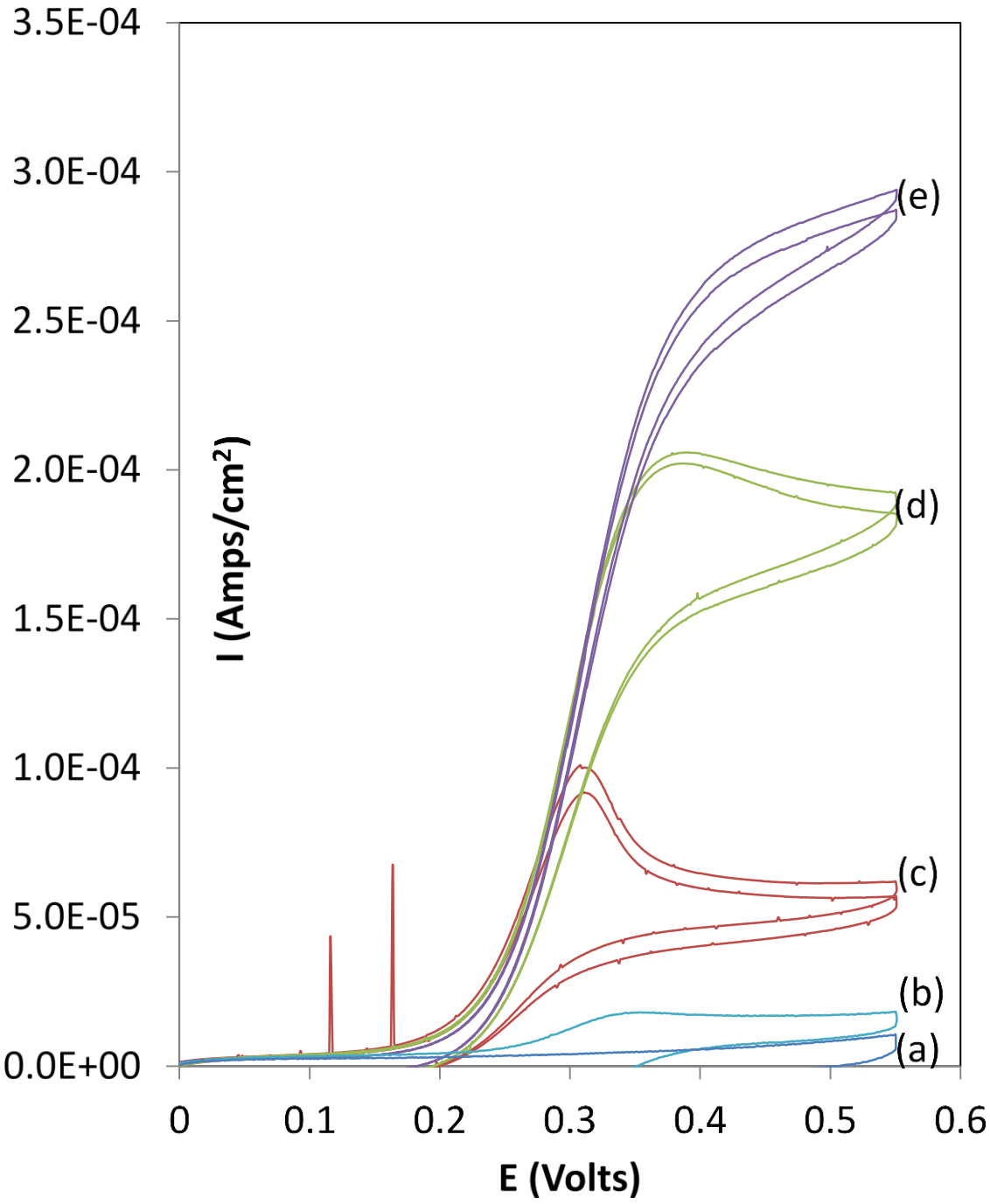

Figure 2

Figure 2. Cyclic voltammograms of the PVA-pphTEOS-SOD graphite electrode in PBS (0.2 M, pH 8.0) (a) in the absence (b) and presence of FMCA (0.8 mM). Curves *c*, *d* and *e* are electrocatalytic responses to the oxidation of sarcosine in PBS (0.2 M, pH 8.0) containing 2.5 (c), 10.0 (d) and 20.0 mM (e) sarcosine, respectively, in the presence of FMCA (0.8 mM). Scan rate of 5 mV s^{-1}.

The electrocatalytic peak current increases by increasing the concentration of sarcosine in buffer solution. These results indicate that the immobilized SOD in PVA-pphTEOS retained its electrocatalytic activity for the oxidation of sarcosine. The reaction at the working or sensing electrode can be described by the following mechanism.

$$FMCA \rightleftarrows FMCA^{+} + e^{-} \quad (4)$$

$$SOD(FAD) + Sarcosine \underset{k_{-1}}{\overset{k_1}{\rightleftarrows}} SOD(FAD\text{-}Sarcosine) \xrightarrow{k_2} SOD(FADH_2) + Glycine + Formaldehyde \quad (5)$$

$$SOD(FADH_2) + 2FMCA^{+} \xrightarrow{k_3} SOD(FAD) + 2FMCA \quad (6)$$

where SOD(FAD and $FADH_2$) represent the oxidized and reduced forms of sarcosine oxidase, and FMCA/$FMCA^{+}$ are the reduced and oxidized forms of ferrocene monocarboxylic acid mediator.

Buffer solutions at various pH values were tested to investigate the effect of varying electrolyte pH varied on the response of the PVA-pphTEOS-SOD electrode between 5.0 and 9.0. Figure 3 shows that the maximum response was obtained at pH 8.0. Therefore pH 8.0 was selected as the optimum pH and all measurements were performed at this pH. This value is in good agreement with most of the data reported in the literature[7-11] suggesting that the host material of PVA-pphTEOS composite film did not alter the structure of SOD thereby providing an effective sensing environment similar to that of native SOD.

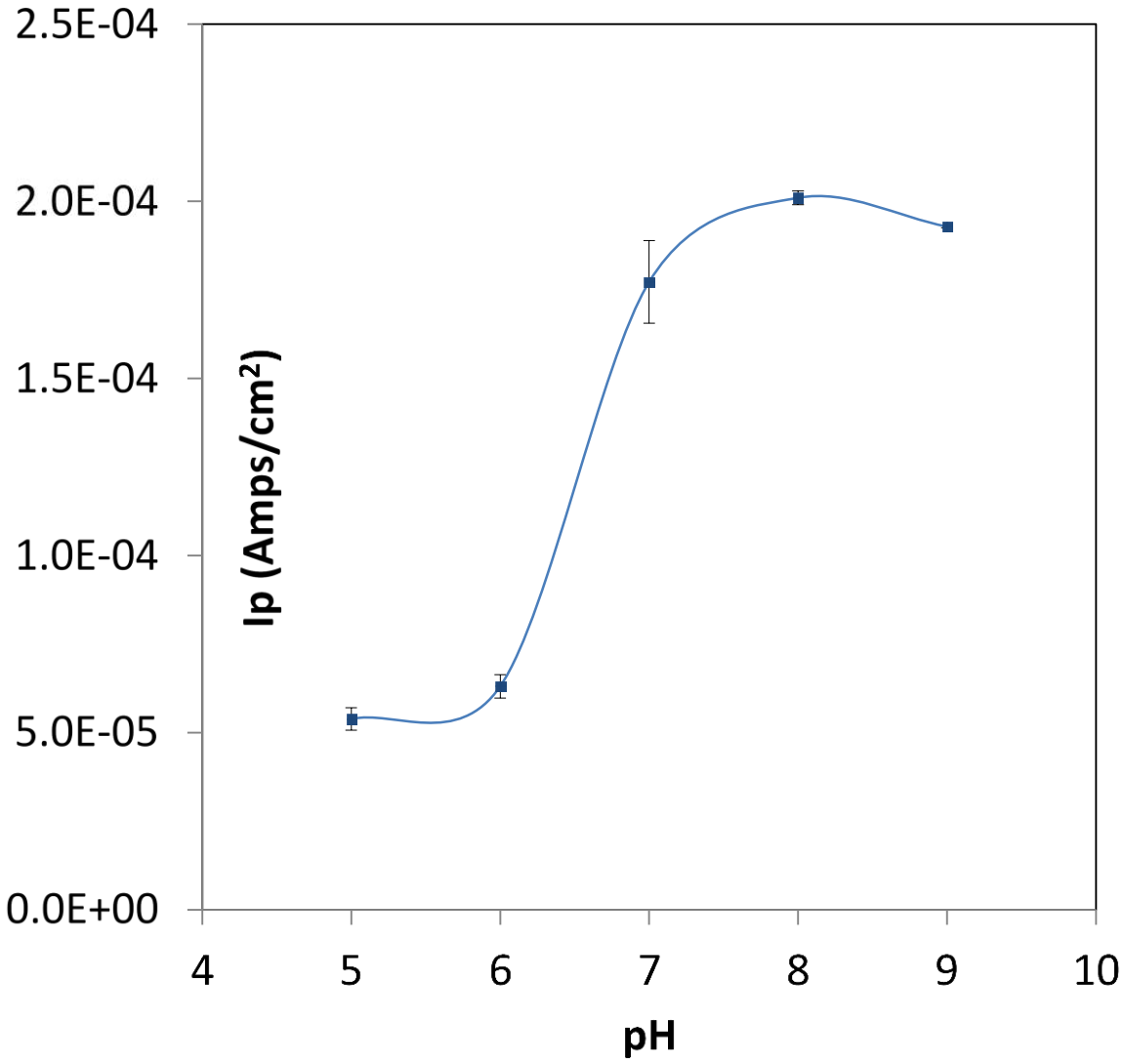

163
164 Figure 3. The effect of buffer pH on current response of the PVA-pphTEOS-SOD electrode.
165

Performance characteristics of the enzyme electrodes. **–** The amperometric *I-t* responses of the PVA-pphTEOS-SOD and PVA-Ag/Au-pphTEOS-SOD electrodes under optimized experimental conditions to successive additions of 0.5 mM sarcosine is shown in Figure 4A. It is clear that relatively rapid and sensitive responses to sarcosine could be achieved for all electrodes apart from those containing AgNPs similar to what we previously reported for immobilized GOD.[6] Calibration curves for the electrodes over the sarcosine concentration range of 0-9 mM are presented in Figure 4B. The average linear range for the electrode of PVA-pphTEOS-SOD was from 1.5 to 6 mM. The respective equation of calibration is I_p = 3.3345 x 10^{-5} $C_{sarcosine}$ + 4.6578 x 10^{-6} with a correlation coefficient of 0.992. The slopes in each case represent the current sensitivity to sarcosine in Amps mM^{-1} cm^{-2}. The limit of detection (LOD) for the enzyme electrode was estimated to be 0.53 mM at a signal-to-noise ratio (*S*/*N*) of 3.

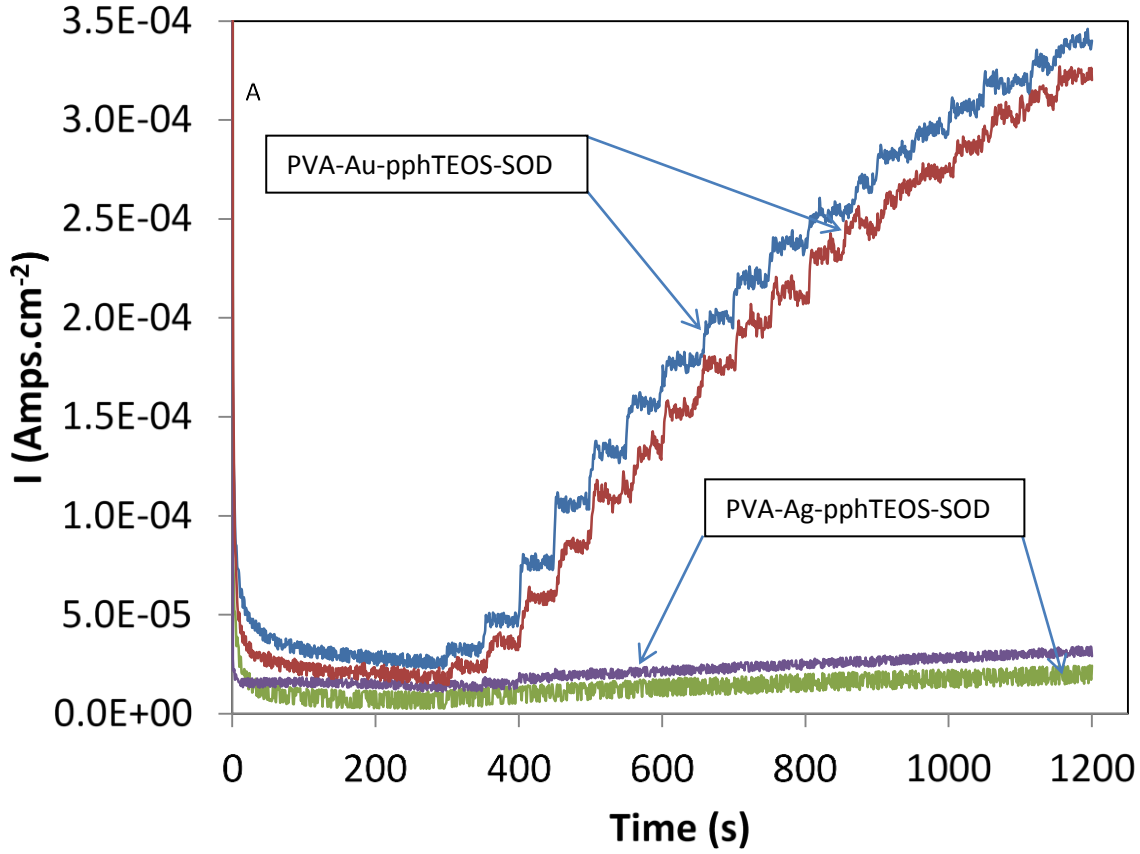

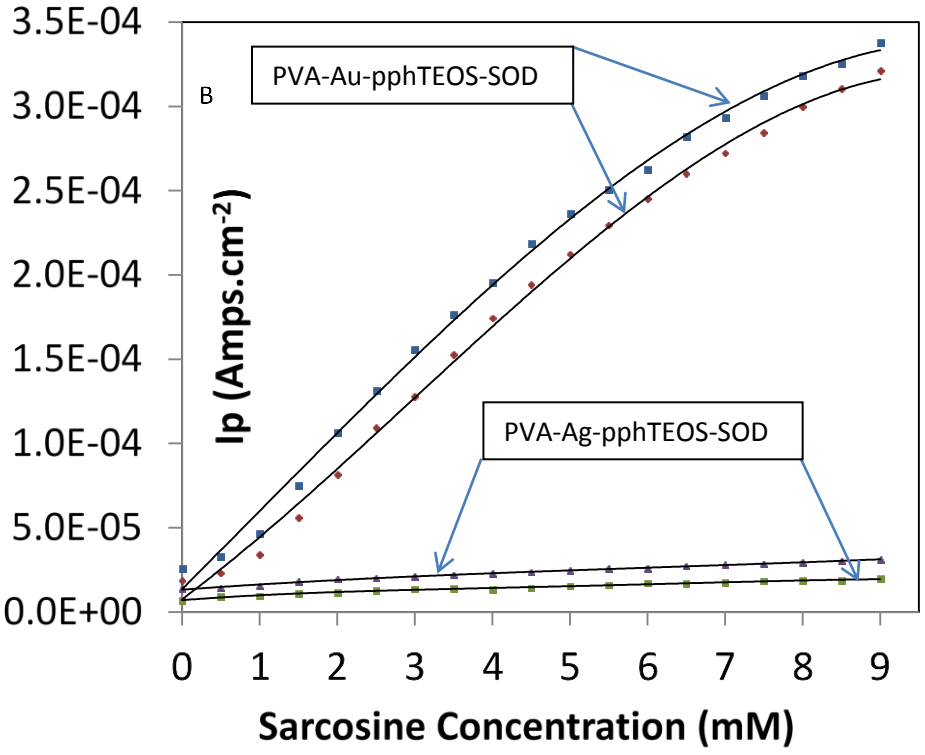

Figure 4A and Figure 4B

176

Figure 4. *Current-time* curves obtained at the PVA-Ag-pphTEOS-SOD (A, *lower* plots), PVA-Au-pphTEOS-SOD (A, *upper* plots) on graphite electrodes for successive additions of 0.5 mM sarcosine. Conditions: 0.2 M pH 8.0 PBS in the presence of 0.8 mM FMCA; applied potential, 0.55 V (*vs.* Ag/AgCl). Plot B show the calibration curves of the enzyme electrode as a function of sarcosine concentrations.

The PVA-pphTEOS-SOD-graphite electrode reached 95% of the steady-state current within an average of 17 s as calculated from each step in the linear region. The slightly high response time can be partially attributed to the loss in enzyme loading due to the precipitation during the preparation of the enzyme-PVA-pphTEOS layer on graphite electrode surface as well as diffusional constraints imposed on the substrate on approach to the active sites of enzyme.

Table I. Summary of the performance characteristics at the amperometric enzyme electrodes.

Parameters	**PVA-pphTEOS-SOD**	**PVA-Au-pphTEOS-SOD**
Linear Range (mM)	1.5-6	0.5-7.5
Sensitivity (Amps cm^{-2} mM^{-1})	3.3345 x 10^{-5}	4.0131 x 10^{-5}
R^2	0.992	0.984
I_{max} (μA)	46.6	66.0
Response Time ($T_{95\%}$, 0.5 → 1 mM, s)	17	8
K_m^{app} (mM)	22.3	16.5
LOD (S/N=3, mM)	0.53	0.5
Reproducibility (RSD)	0.84%	-

Figure 4A shows the amperometric *I-t* responses of the PVA-Ag-pphTEOS-SOD and PVA-Au-pphTEOS-SOD electrodes, where the latter electrode displayed nearly linear, reproducible and highly sensitive response to changes in sarcosine concentration from 0.5-7.5 mM. The respective equation of calibration for PVA-Au-pphTEOS-SOD is I_p = 4.0131 x 10^{-5} $C_{sarcosine}$+ 2.4294 x 10^{-5} with correlation coefficient of 0.984, which suggests that in the presence of AuNPs the sensitivity is improved by 20%. The LOD for the enzyme electrode was estimated to be 0.5 mM at a signal to noise ratio (*S*/*N*) of 3, only slightly lower than electrodes without the AuNPs.

The PVA-Au-pphTEOS-SOD graphite electrodes reached 95% of the steady-state current within an average of 8 s, as calculated from each step in the linear region shown in Figure 4A. The presence of AuNPs greatly improved the response time, as well as the activity of SOD. The micro-environment and stability of the enzyme was found to be clearly improved in the presence of the NPs.

The PVA-Ag/Au-pphTEOS-SOD graphite electrodes were also tested under cyclic voltammetric conditions in PBS over the apparent direct electron transfer potential range for SOD. Although the sarcosine detection characteristics were improved with the presence of AuNPs, no response was seen to signify direct

electron transfer from SOD as others have reported for other FAD containing enzymes.[12-18] As previously reported, the improvement in response can be a result from the large active surface areas and the excellent electron transfer ability of the AuNPs, but not great enough to penetrate the enzymes' protein shell and develop direct connectivity. The presence of AgNPs showed an extremely degenerative response to sarcosine. This was suspected to be caused by the heavy metal Ag^{+} ions unreacted in the silver colloid.[19]

The apparent Michaelis-Menten constant (K_m^{app}) can be calculated from the electrochemical version of the Linweaver-Burk equation:

$$1/I_{ss} = 1/I_{max} + K_m^{app} / I_{max} \times C \quad (7)$$

where I_{ss} is the steady-state current after the addition of substrate, I_{max} is the maximum current under saturated substrate conditions, C is the concentration of substrate. The K_m^{app} value for the PVA-pphTEOS-SOD and PVA-Au-pphTEOS-SOD electrodes was found to be 22.3 mM and 16.5 mM respectively, which is relatively high compared to that of the native enzyme.[7, 8] In addition, this is also high compared to other research reports in this area.[5, 10, 11] This can be attributed to the highly robust nature of the interlinked PVA and pphTEOS matrix, which imposes diffusional constraints on the substrate to the enzyme active site. In addition, the slight precipitation occurring in the enzyme mixture suggests that the enzyme could have been moderately denatured resulting in lower activity and low affinity towards sarcosine. However, in the presence of AuNPs, the value of K_m^{app} is much lower signifying an improvement in the microenvironment of the enzyme and conductivity within the PVA-pphTEOS matrix.

Reproducibility and Stability of the Enzyme Electrode. – Several calibration curves were plotted using independently prepared PVA-pphTEOS-SOD electrodes. The reproducibility (RSD) of their sensitivities was found to be 0.84%. This indicated that the electrodes were extremely reproducible in terms of multiple electrode preparations and testing from time to time during the laboratory measurements.

The immobilization of SOD by the entrapment in a PVA-pphTEOS composite film was quite stable. When the PVA-pphTEOS-SOD graphite electrode was scanned continuously in a solution of sarcosine in the presence of FMCA mediator, the voltammetric response decreased slowly with a slight peak at around the 20th cycle where the matrix was assumed to have swollen leading to higher accessibility of the substrate before slow leaching of SOD. The peak current remained around 82% of the initial response after 50 cycles. This clearly suggested that the sensing electrode remains highly active for prolonged periods in a multiple test campaign. Table I shows a summary of the key characteristics of the PVA-pphTEOS-SOD and PVA-Au-pphTEOS-SOD graphite electrode derived from the data presented in Figure 4A and 4B.

Conclusion

In this study, SOD was successfully immobilized in PVA and pphTEOS matrix, in the absence and in the presence of Ag or AuNPs, on a graphite electrode and the performance characteristics of the resulting enzyme electrodes investigated. The PVA-pphTEOS-SOD enzyme electrode presented a good linear range, sensitivity and LOD for the detection of sarcosine. In addition, it also showed excellent reproducibility. Where AgNPs created a detrimental effect on the determination of sarcosine, AuNPs however, led to significant improvements in the response times and K_m^{app} value. The linear range was also extended and sensitivity increased. Incorporation of AuNPs within the PVA-pphTEOS created a more favourable environment for SOD thereby increasing its affinity towards sarcosine and activity. The successful immobilization of SOD acts as a model to what could potentially be a creatinine based biosensor as most of the fundamental chemistry of the three enzyme system happens at the redox site of SOD which will be demonstrated in our future research publication.

Acknowledgements

The authors wish to thank EPSRC for the DTA award to UL and British Council UK funding part of the research work on hybrid thin films in collaboration with Bulgaria. UL also wishes to thank SPEME/IMR for the infrastructure support during the course of this research work.

Reference

1. U. Lad, S. Khokhar and G. M. Kale, *Anal. Chem.*, **80**, 7910 (2008).
2. T. Tsuchida and K. Yoda, *Clin. Chem.*, **29**, 51 (1983).
3. A. E. G. Cass, G. Davis, M. J. Green and H. A. O. Hill, *J. Electroanal. Chem.*, **190**, 117 (1985).
4. I. Taniguchi, S. Miyamoto, S. Tomimura and F. M. Hawkridge, *J. Electroanal. Chem.*, **240**, 333 (1988).
5. Y. Zhou, H. Yin, X. Meng, Z. Xu, Y. Fu and S. Ai, *Electrochim. Acta*, **71**, 294 (2012).
6. U. Lad, G. M. Kale and R. Bryaskova, *Anal. Chem.*, **85**, 6349 (2013).
7. V. K. Nguyen, C. M. Wolff, J. L. Seris and J. P. Schwing, *Anal. Chem.*, **63**, 611 (1991).
8. S. Hayashi, M. Suzuki and S. Nakamura, *Biochim. Biophys. Acta*, **742**, 630 (1983).
9. A. Ramanavicius, *Anal. Bioanal. Chem.*, **387**, 1899 (2007).
10. Y. Yang and S. Mu, *J. Electroanal. Chem.*, **415**, 71 (1996).
11. Y. Shi, Y. Yang, J. Kan, S. Mu and Y. Li, *Biosens. Bioelectron.*, **12**, 655 (1997).
12. Y. Xiao, F. Patolsky, E. Katz, J. Hainfeld, F and I. Willner, *Science*, **299**, 1877 (2003).
13. H. Ju, S. Liu, B. Ge, F. Lisdat and F. W. Scheller, *Electroanal.*, **14**, 141 (2002).
14. J. Zhao, R. W. Henkens, J. Stonehuerner, J. P. O'Daly and A. L. Crumbliss, *J. Electroanal. Chem.*, **327**, 109 (1992).
15. K. R. Brown, A. P. Fox and M. J. Natan, *J. Am. Chem. Soc.*, **118**, 1154 (1996).
16. X. Yi, J. Huang-Xian and C. Hong-Yuan, *Anal. Biochem.*, **278**, 22 (2000).
17. H.-Y. Gu, A.-M. Yu and H.-Y. Chen, *J. Electroanal. Chem.*, **516**, 119 (2001).
18. S.-Q. Liu and H.-X. Ju, *Anal. Biochem.*, **307**, 110 (2002).
19. S. Ma, W. Lu, J. Mu, F. Liu and L. Jiang, *Colloids Surf., A*, **324**, 9 (2008).